



## A new data analysis approach for an AgNPs-modified impedimetric bioelectronic tongue for dairy analysis

C. Perez-Gonzalez<sup>a,c</sup>, C. Salvo-Comino<sup>a,b</sup>, F. Martin-Pedrosa<sup>b,c</sup>, M.L. Rodriguez-Mendez<sup>a,b,\*\*</sup>,  
C. Garcia-Cabezon<sup>b,c,\*</sup>

<sup>a</sup> Group UVASENS, Escuela de Ingenierías Industriales, Universidad de Valladolid, Paseo del Cauce, 59, 47011, Valladolid, Spain

<sup>b</sup> BioecoUVA Research Institute, Universidad de Valladolid, 47011, Valladolid, Spain

<sup>c</sup> Dpt. of Materials Science, Universidad de Valladolid, Paseo del Cauce, 59, 47011, Valladolid, Spain

### ARTICLE INFO

#### Keywords:

Biosensor  
Electronic tongue  
Impedimetric sensor  
Milk  
Nanoparticles

### ABSTRACT

An alternative approach to analyze complex matrices, such as milk, lies on multivariate description of the chemical composition of samples, where fingerprints for each sample are generated using data mining methods (Principal Component Analysis, PCA, and Supported Vector Machine). Electronic tongues (ET) hold substantial potential for the dairy industry as analytical tools due to their fast analysis. The purpose of this work was to create an impedimetric ET with an array of microelectrode sensors for application in the dairy industry. A sensor array with enhanced sensitivity and selectivity silver nanoparticles and enzymes were developed. Higher sensitivity was evident in the responses of this array to milk components of interest like glucose, galactose, lactose, and urea. PCA of the signals obtained using the optimized ET has allowed the discrimination of milks with different characteristics. SVM was used to establish correlations between the signals obtained from the ET and the physicochemical parameters. Electrochemical Impedance Spectroscopy have also shown that the ET in combination with the equivalent circuits approach could be a potential tool for its further application in dairy analysis. Moreover, the study of milk samples confirmed the high cross-selectivity of the system which allowed the development of classification models and to establish correlations between the ET and physicochemical parameters.

### 1. Introduction

Simultaneous detection of multiple species of interest in complex liquid samples is one of the challenges faced in the development of sensors arrays for food quality control in recent years. Several approaches have been made to the detection of electroactive species, such as phenols and antioxidants, with voltammetric and potentiometric sensors developing electronic tongues (Garcia-Hernandez, Salvo-Comino, Martin-Pedrosa, Garcia-Cabezon, & Rodriguez-Mendez, 2020; Sobrino-Gregorio, Bataller, Soto, & Escriche, 2018; Sun et al., 2023). However, these ET have not shown efficient results for non-electroactive species that account for a significant portion of the composition of food matrices.

The use of Impedimetric electronic tongues could be an excellent solution to this issue. Electronic tongues (ET) based on impedance spectroscopy, can be used to determine interfacial interactions on the

sensor surface performing non-destructive measurements. Furthermore, unlike other electrochemical techniques, impedance spectroscopy do not always require a reference electrode or sensing units containing electroactive materials or active species in the sample allowing detection of charged and uncharged species (Kelcilene, Shimizu, Scagion, & Correa, 2019; bib\_kelcilene\_et\_al\_2019).

ET based on electrochemical impedance spectroscopy (EIS) technique were initially developed by Riul et al. These were based on the application of a sinusoidal signal along a wide range of frequencies for a fixed amplitude. Applying sinusoidal signals (from 20 Hz to 100 kHz) to interdigitated electrodes coated with chemosensitive materials allowed the discrimination between standard solutions including sucrose, sodium chloride and potassium chloride (Riul, Malmegrim, Fonseca, & Mattoso, 2003).

The use of interdigitated microelectrodes has radically revolutionized EIS research. These microelectrodes have great advantages due to

\* Corresponding author. BioecoUVA Research Institute, Universidad de Valladolid, 47011, Valladolid, Spain.

\*\* Corresponding author. Group UVASENS, Escuela de Ingenierías Industriales, Universidad de Valladolid, Paseo del Cauce, 59, 47011 Valladolid, Spain.

E-mail addresses: [mluz@uva.es](mailto:mluz@uva.es) (M.L. Rodriguez-Mendez), [crigar@uva.es](mailto:crigar@uva.es) (C. Garcia-Cabezon).

their low electric resistance, high signal-to-noise ratio, shorter times until steady state, and smaller sample requirements. In addition, they can easily be modified with biological and sensitive materials. For instance, strategies based on the modification with nanomaterials such as metal nanoparticles has been reported (Manzoli et al., 2014; Mercante et al., 2015). Moreover, the binding of biomolecules to these microelectrodes modifies the interfacial properties and the effective variations in impedance values can be used to quantify enzyme processes (Eugenii & Willner, 2003).

EIS-based interdigitated microelectrodes can be classified into two categories: faradaic and non-faradaic EIS, i.e. in presence of a redox probe used as a marker or directly in an analyte solution respectively. The non-faradaic sensors mainly depend on the capacitance change on the interface between electrode-electrolyte. Meanwhile faradaic sensors register charge transfer processes associated to electrochemical oxidation/reduction processes on the electrode surface (Daniels & Pourmand, 2007). By controlling the current generated from the redox reactions, the faradaic sensors can achieve higher sensitivity (Tolga, Ates, & Sarac, 2016; Park et al., 2018). However, faradaic biosensors provide fast responses and have great specificity for target molecules with high sensitivities by detecting changes in the transfer process between the electrode and redox probe (Park J. et al., 2018). They also have disadvantages such as their sensitivity to external influences, which implies the need of using Faraday boxes to reduce system noise, or the challenges associated to reproducibility (Luka et al., 2015).

The efficiency of impedimetric ET in the food industry has been proven on the discrimination of several water contaminants such as heavy metals, toxins, pesticides, and medicines (Hui et al., 2013; Wang et al., 2013; Kelcilene, Flávio, Scagion & Correa D.S. 2019; Manzoli et al., 2014; Murilo, Mercante, Mattoso, & Correa, 2017; Wania et al., 2021). It has also been applied in food control through its use for the determination of phenolic species in must and wine samples (Garcia-Hernandez, Salvo Comino, Martín-Pedrosa, Rodriguez-Mendez, & Garcia-Cabezon, 2018), to determine physicochemical properties such as salt and moisture content in meats (Masot et al., 2010), to analyze the freshness of seafood (Swatland, Darkin, Naylor, Caston, & Moccia, 1998), the degree of curing in cheeses (Kelcine et al., 2019), or for honey samples classification based on their origin (Ulloa et al., 2013). However, there are not many studies using impedimetric ETs for milk sample characterization due to the complexity of the matrix.

Shrikrishnan et al. demonstrated that bovine milk contains different species that can be detected without the need for an electrolyte support by electron transfer studies using redox probes with different physicochemical characteristics (Shrikrishnan & Lakshminarayanan, 2012). Additionally, EIS techniques had been used to evaluate the bacteriological quality of milk (Joung et al., 2013, Wan, Ping, Ye, Wu & Ying 2013), milk adulteration (Goran et al., 2021; Siuli, Sivaramakrishna, Biswas, & Goswami, 2011) and to determine different milk fat contents (Veiga & Bertemes-Filho, 2012). Impedimetric ETs have also been used to characterize ultra-pasteurized milk (Lopes, Machado, Ramalho, & Silva, 2017) or for antibiotics detection (Vanessa et al., 2016).

The performance of ETs could be enhanced by creating systems designed to identify specific components. Bioelectronic tongues (bio-ETs), combining unspecific sensors with biological receptors such as enzymes, have supposed a great advance in the development of electrochemical sensors, since they provide global information and specific information about compounds targeted by the enzymes (Skládal, 2020). The introduction of biosensors in dairy products could give quantitative and qualitative data about non-electrochemical species such as sugars, proteins or triglycerides. Considering the importance of surface interactions in EIS, this could be a great advantage in the discrimination of milk samples with really similar compositions. Furthermore, impedimetric bio-ETs can be improved by combining enzymes with nanomaterials, which provides an effective immobilization of the biomolecules while preserving or even enhancing their biological activity (Govindhan & Jin, 2017; Reis et al., 2014).

Different nanomaterials such as carbon nanotubes (Govindhan & Jin, 2017), phthalocyanines (Reis et al., 2014) and metallic nanoparticles (Xiliang et al., 2006; Pérez-González, Salvo-Comino, Martín-Pedrosa, García-Cabezón, & Rodríguez-Méndez, 2023) have proven to enhance the immobilization of enzymes, favouring the electrocatalytic activity of the sensors. Migliorini et al. developed a novel urea impedimetric biosensor using polymeric electrospun nanofibers of polyamide that showed excellent properties for the immobilization of urease, conferring the electrode high sensitivity with a limit of detection of 0.011 mg dL<sup>-1</sup> (Fernanda et al., 2018). However, there have only been a few reports of impedimetric bio-ETs that combine metallic nanoparticles and enzymes. The development and study of the capabilities of multisensory systems containing combinations of enzymes and nanomaterials is a new field of research. An array of sensors based on electrospun conducting polymers nanofibers deposited onto interdigitated electrodes was used for detecting tetracycline in milk samples (Vanessa et al., 2016).

The objective of this research is to create an impedimetric bio-electronic tongue and a new data analysis approach for EIS that could be applied in the analysis of complex matrices, such as milk samples, using a combination of parallel-operating microelectrode-based biosensors. In order to enhance the sensor sensitivity, silver nanoparticles (AgNPs) are deposited on the sensor surface. Due to their electrochemical properties, silver nanoparticles (AgNPs) can be a great choice to improve the performance of biosensors, their high electrical conductivity, and their ability to amplify bio electrochemical signals (Salvo-Comino et al., 2022; Sandeep, Santhosh, Swamy, Suresh, & Melo, 2019, Ali Saad, Wadood, & Ali, 2019). Additionally, to improve the sensors selectivity, enzymes including galactose oxidase, glucose oxidase, beta-galactosidase, urease and lipase were immobilized. The system is applied for discrimination and classification purposes by using principal components analysis and support vector machine.

## 2. Methodology

### 2.1. Reagents and solutions

Silver nitrate (AgNO<sub>3</sub>), phosphate buffer, Nafion® 117, the enzymes galactose oxidase (GaOx) (from *Dactylium dendroides*), glucose oxidase (GOx) (from *Aspergillus niger*), β-galactosidase (β-Gal), (from *Aspergillus oryzae*), urease (Ure) (from *Canavalia ensiformis*) and lipase (Lip) (from *Candida Rugosa*) were acquired in Sigma-Aldrich (Saint Louis, MO, USA). All the solutions were prepared in deionized water from MilliQ (Millipore of Sigma Aldrich, Darmstadt, Germany). Potassium chloride (KCl) was acquired by PanReac AppliChem (Barcelona, Spain) and NaBH<sub>4</sub> 98% from Alfa Aesar (Haverhill, MA, USA).

Gold thin-film interdigitated (IDE) sensors were purchased from MicruX Technologies. Silver nanoparticles (AgNPs, 20–30 nm) were synthesized according to the procedure proposed by Slot and Geuze (Creighton, Blatchford, & Albrecht, 1979).

### 2.2. Sensors and biosensors development

Sensors were prepared utilizing gold IDE sensors as substrates (2 mm electrochemical cell surface) with a three electrodes system: working electrode (WE1), reference electrode (RE) and auxiliary electrode (AE). The working electrode was made out of two individually addressable arrays of microelectrodes with an interdigitated approach. The reference electrode was used in order to ensure that all tests were performed at proper potential.

Prior to the nanoparticles deposition, substrates were washed in an ultrasonic bath and rinsed twice with deionized water.

Silver nanoparticles were deposited onto the IDE sensor by drop-casting 20, 30 or 40 μL of the AgNPs suspension (2 g/L AgNPs). After drying, 20 μL of the enzyme (5 g/L GOx, GaOx, β-Gal, Ure and Lip suspended in phosphate buffer 0.1 M, pH 7.0) were deposited by drop-cast onto the electrode surface. Finally, 20 μL of Nafion on a

concentration of 1:3 in ethanol was drop-casted on top of both ensuring their correct immobilization. All sensors were stored at 4 °C prior to use.

All enzymes (GOx, GaOx,  $\beta$ -Gal, Ure and Lip) were used at active pH (optimum 7.5, 7, 6 and 7.5 respectively).

### 2.3. Characterization of the sensors

UV-Vis and Transmission electron microscopy (TEM) were used in the AgNPs characterization with a UV-2600 device (Shimadzu, Duisburg, Germany) and Transmission TEM JEM 1011 H R. Atomic force microscopy (AFM) was used to determine the sensors topography in a Cypher ES Environmental AFM device functioned on tapping mode with blue drive photothermal and tip AC160TSA-R3 (Oxford Instruments, Asylum Research, Wiesbaden, Germany).

Electrochemical measurements were performed on a potentiostat-galvanostat PGSTAT128 (Autolab Metrohm, Utrecht, The Netherlands). The impedance spectroscopy was carried out by applying a 10 mV signal amplitude, on frequencies from 0.1 to 1000 Hz. Measurements were made in six electrolytes:  $[\text{Fe}(\text{CN})_6]^{4-/3-}$  (5 mmol L<sup>-1</sup>), phosphate buffer (0.1 mol L<sup>-1</sup>), galactose, glucose, lactose, urea (0.1, 0.01 and 0.001 mol L<sup>-1</sup>) and diluted milks in 4:1 in  $[\text{Fe}(\text{CN})_6]^{4-/3-}$  (5 mmol L<sup>-1</sup>). Impedance spectra were fitted using Zview2 software, Scribner Associates, Inc. Ten replicas per milk sample were carried out.

Voltammetric measurements were registered on a potential range from -1 to +1 V<sub>Ag/AgCl</sub>, with a scan rate of 100 mV/s and a potential step of 10 mV.

### 2.4. Milk samples

In this work 90 milk samples corresponding to 9 types of commercial ultra-pasteurized milk were studied. This set was sorted by their fat percentage (whole, semi-skimmed and skimmed milk) and by their specific nutritional characteristics (lactose-free and calcium-enriched milk). All the samples were analyzed using standard chemical methods following the international standardized methods: the Tritation method for acidity, hydrometer method for density, Gravimetry Röse-Gottlieb method for fat content, Kjeldahl method for protein content, HPLC to determine lactose content and infrared spectroscopy for urea, non-fat dry matter (NFDM) and dry matter (DM) (IOFS 2021). The summary of the chemical analysis are collected in Table 1.

### 2.5. Electronic tongue measurements

The impedimetric measurements were carried out by depositing 50  $\mu$ l of the milk sample on the sensors surface after which a test was performed at open circuit potential for 10 min to ensure sample stabilization. Impedance spectroscopy was carried out at frequencies between 0.1 Hz and 10<sup>5</sup> Hz at an intensity of 10 mA. Between samples the sensors were cleaned by immersion in deionized water under agitation.

**Table 1**  
Milk samples physicochemical parameters determined by traditional standard methods.

Sample	Fat content	Nutritional description	Acidity (°D)	Density (g/ml)	Fat (% m)	Proteins (% m)	Lactose (% m)	Urea (mg/ml)	NFDM (% m)	DM (% m)
M1	Skimmed	Classic	12.55	1031.55	0.31	3.3	5	387	9.02	9.33
M2	Skimmed	Calcium	15.82	1039.47	0.29	3.93	5.59	724	10.51	10.8
M3	Skimmed	Lactose Free	12.66	1033.57	0.32	3.29	0.36	<10	9.02	9.33
M4	Semi-Skimmed	Classic	12.55	1031.6	1.56	3.27	4.91	355	8.91	10.47
M5	Semi-Skimmed	Calcium	16.06	1037.29	1.55	3.9	5.49	597	10.40	11.95
M6	Semi-Skimmed	Lactose Free	12.19	1032.09	1.59	3.31	0.42	<10	8.99	10.57
M7	Whole	Classic	12.17	1029.38	3.56	3.21	4.85	388	8.78	12.33
M8	Whole	Calcium	15.86	1035.71	3.55	3.91	5.54	769	10.45	14.0
M9	Whole	Lactose Free	11.98	1029.4	3.59	3.23	0.31	<10	8.82	12.41

### 2.6. Chemometrics

EIS measurements were processed on Matlab R2020a (The Mathworks Inc., Natick, USA) and OriginPro2020 (Origin Lab Northampton, Massachusetts, USA). The impedance curves were adjusted to equivalent circuit using Zview2 software prior to their use as data source for statistical analysis. Principal Component Analysis (PCA) was applied to evaluate the discrimination capability of the bioET as an unsupervised methodology using Matlab R2020a (The Mathworks Inc., Natick, USA). To establish correlations between the signals obtained from the bioET and the physicochemical parameters provided by standard methods Support vector machine (SVM) was used on Matlab R2020a (The Mathworks Inc., Natick, USA).

## 3. Results and discussion

### 3.1. Structural characterization

First, the characterization of the silver nanoparticles was carried out using UV-Visible spectroscopy (Fig. 1). The absorption spectrum obtained from the colloidal solution of metallic nanoparticles shows an intense and narrow absorption peak can be observed at a wavelength of 418 nm that coincides with the absorption spectrum of the resonance plasmon of silver confirming the presence of AgNPs. In addition, TEM micrographs (Fig. 1B) showed the formation of well-dispersed silver nanoparticles with an approximately diameter of 20  $\pm$  10 nm.

AFM pictures of the IDE electrodes covered with AgNPs and the combination of the nanoparticles with an enzyme are illustrated in Fig. 1C and 1D. As it can be observed, AgNPs showed spherical forms with a 20–10 nm average diameter. These structures are homogeneously distributed along the electrode surface ensuring the correct interaction between the nanomaterial and the tracks. Only few nanoparticle clusters were identified. The size of the nanostructures increased as the enzymes were immobilized. This was illustrated in Fig. 1D where the topographic images of glucose oxidase deposited onto AgNPs are shown. As observed in the figure, the roughness of the surface, measured as the average diameter of the structures, significantly showing structures up to 45  $\pm$  10 nm. These results confirm the correct immobilization of the enzyme on the electrode surface.

### 3.2. Electrochemical characterization

The effect of the AgNPs on the electrocatalytic activity of the electrodes was investigated by electrochemical measurements such as cyclic voltammetry and EIS using  $[\text{Fe}(\text{CN})_6]^{4-/3-}$  as a redox probe.

The voltammetric response of the IDE electrodes prepared with increasing volumes of nanoparticles (20, 30 and 40  $\mu$ L of the AgNPs) in a solution of 5 mM the  $[\text{Fe}(\text{CN})_6]^{4-/3-}$  can be observed in Fig. 2A. All signals showed oxidation and reduction peaks at E<sub>a</sub> = 400 mV and E<sub>c</sub> = -450 mV respectively near to the redox pair of the  $[\text{Fe}(\text{CN})_6]^{4-/3-}$

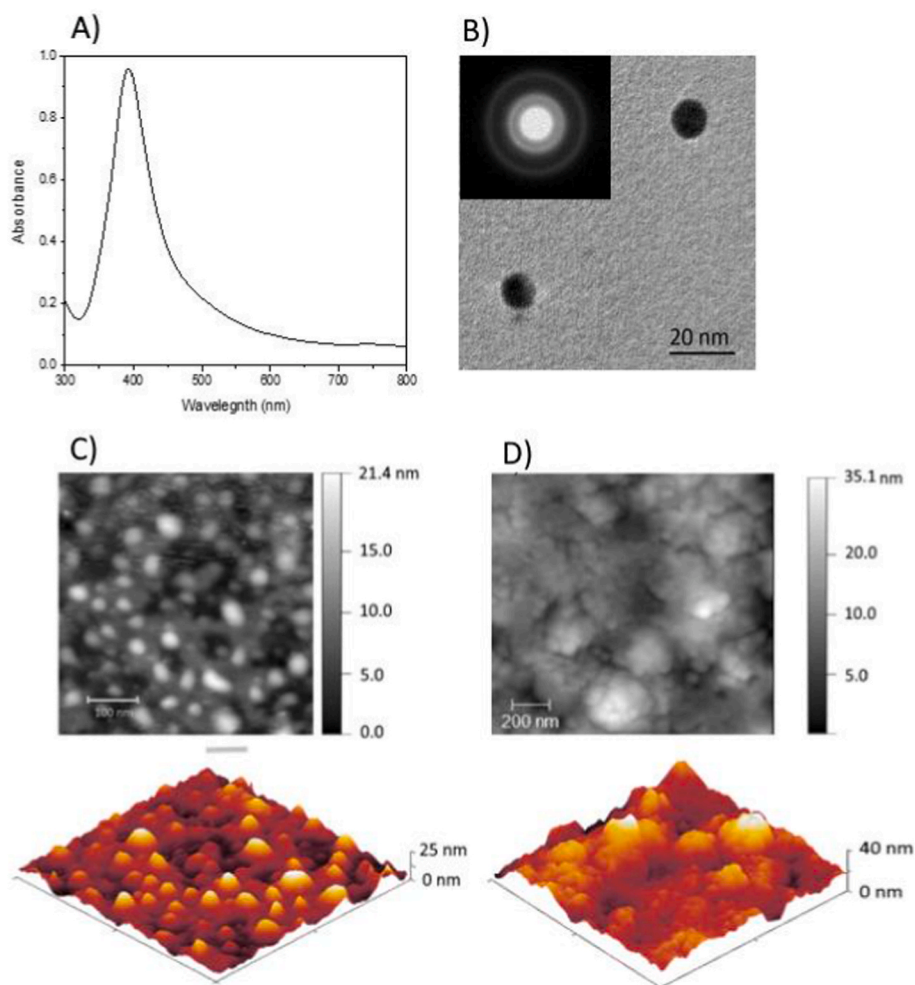


**Fig. 1.** Characterization of AgNPs. A) UV-Vis absorption spectra, B) TEM micrograph and ED pattern. C) AFM characterization of the sensor surface IDE-AgNPs D) AFM characterization of the sensor surface IDE-AgNPs-GaOx.

couple. The responses of the AgNPs sensor showed higher peak intensities when the amount of AgNPs is increased from 20 to 30 and 40  $\mu\text{l}$  compared with the bare electrode. This behaviour shows how the deposition of nanoparticles on the surface of the electrodes favours the electrocatalytic activity. It can also be observed a slight displacement of the redox couple towards a lower voltage with the increase of AgNPs, which would indicate a greater reversibility of the system.

The enhancement of the electrochemical response was similar to the response reported in previous works where silver nanomaterials have been used as electron transfer mediators in sensors technologies (Coral-Salvo et al., 2022). As increasing amounts of AgNPs are deposited, the conductivity becomes more intense. This behaviour is likely due to the AgNPs' increased effective surface area.

The impedimetric response of the IDE electrodes prepared with increasing volumes of nanoparticles (20, 30 and 40  $\mu\text{l}$  of the AgNPs) was also studied (Fig. 2B and 2C). The impedance measurements were performed at a fixed circuit potential. The Nyquist plots (Z real vs. Z imaginary) registered showed a semi-circular shape in the high-frequency region. The diameter of the semicircle is proportional to the electron transfer resistance ( $R_{ct}$ ) in this region, which relates to electron-transfer processes. For faradaic EIS,  $R_{ct}$  serves as the primary parameter for describing the electrochemical process on the sensor surface. Conversely, non-conductive molecules block the electron transfer mechanism leading to an increase of the  $R_{ct}$ .

In experiments performed with increasing quantities of AgNPs, it was observed that the diameter of the semicircle changed with the amount

added. Fig. 2B illustrates the obtained curves. Sensors without modification showed wider curves corresponding with a higher electron transfer resistance compared to sensors modified with AgNPs. Furthermore, increasing amounts of AgNPs showed progressive lower  $R_{ct}$  values indicating that charge transfer rates were higher due to the efficient electrocatalytic properties of the nanomaterial. Bode diagrams (Fig. 2C), showed that the impedance module was also reduced as the volume of nanoparticles increased while the phase angle for the maximum amount of AgNPs studied showed a shift towards lower frequency values.

The improvement of the observed performance can be attributed to the improved electron transfer rate provided by the AgNPs due to their interactions with the electron surface. For this reason, from this point it was decided to modify the sensors with the maximum volume of nanoparticles tested (40  $\mu\text{l}$ ).

The EIS characteristics of the biosensors were also studied analysing the responses towards standard solutions of the target analytes (for glucose, galactose, lactose and urea).

An important observation was that the semicircle diameter decreased along the sequence IDE-AgNPs-GaOx < IDE-GaOx < IDE (Fig. 3A). The smaller diameter of the curves ( $R_{ct}$ ) revealed the lower electronic transfer resistance which might be produced by the synergetic effect between enzyme activity and the electrocatalytic nanomaterial. This behaviour has also been observed on all the biosensors developed in this work.

The effect of the combination of AgNPs and enzymes in the response towards increasing concentrations of target analytes was also studied

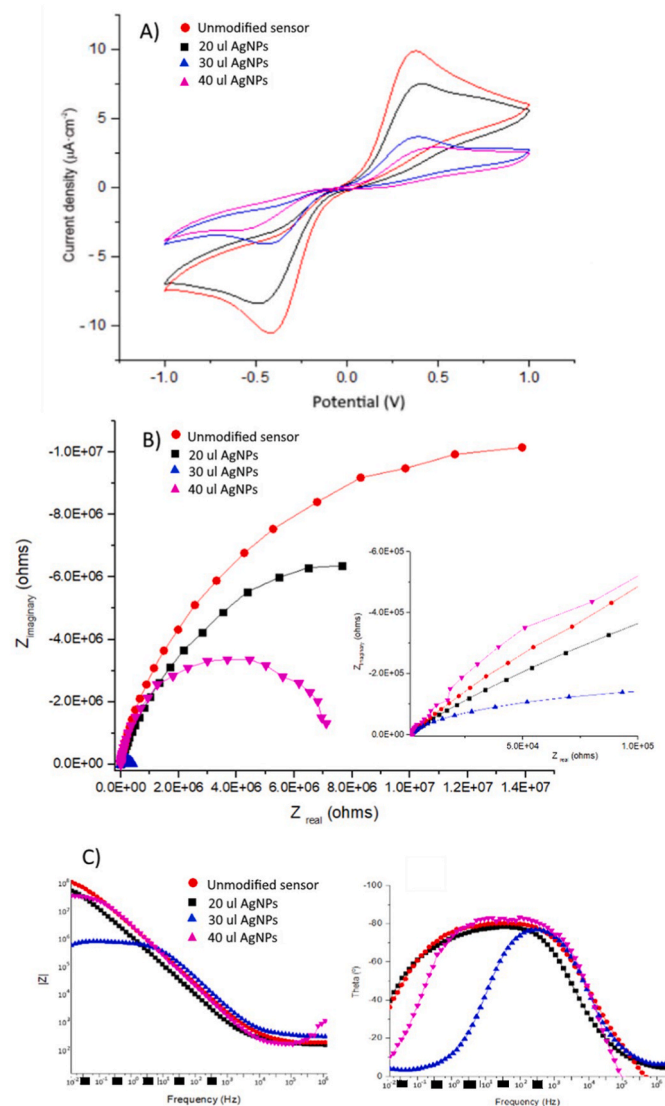


**Fig. 2.** A) Voltammetric response towards the 5 mM  $[\text{Fe}(\text{CN})_6]^{4-/3-}$  of bare sensor and sensors modified with 20, 30 and 40  $\mu\text{l}$  of AgNPs. B) Nyquist diagram and C) Bode diagrams of sensors with 20, 30, 40  $\mu\text{l}$  (blue) of AgNPs and unmodified in 0.1M potassium ferrocyanide.

(Fig. 3B and 3C). Taking as an example the case of IDE-GaOx and IDE-AgNPs-GaOx sensor, it can be observed that the Nyquist diagram have a bigger diameter of semicircle in the absence of AgNPs, due to a greater resistance to electron transfer as a consequence of enzyme coupling

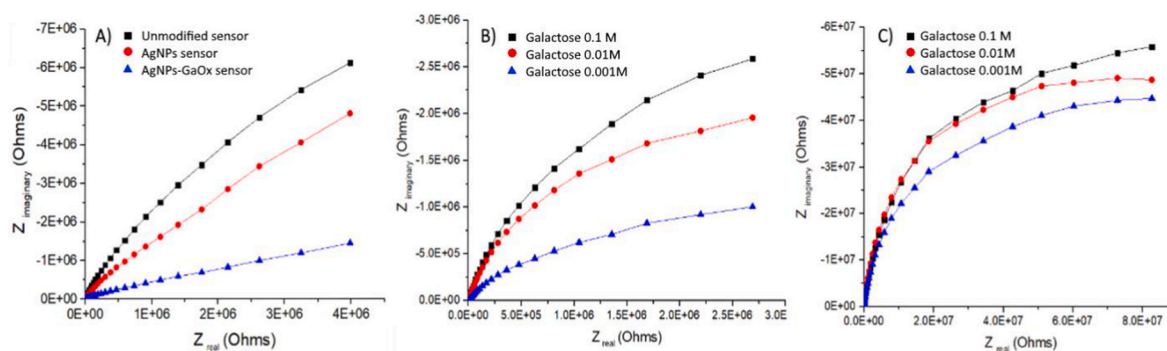


**Fig. 3.** Nyquist diagrams for A) an unmodified sensor, with AgNP and with AgNP-GaOx in galactose 0.1 M, B) sensor with AgNPs-GaOx in galactose 0.1M, 0.01M and 0.001M, and C) sensor with GaOx in Galactose 0.1M, 0.01M and 0.001M.

which is a non-conducting molecule. Moreover, the differences between the impedance measurements are much higher in IDE-AgNPs-GaOx than IDE-GaOx, which confirms the synergic effect of AgNPs-Enzymes in the presence of their target molecule.

In both cases, the analyzed solutions are ordered according to their concentration from highest to lowest (0.1, 0.01 and 0.001  $\text{M}^{-1}$ ) while the  $R_{ct}$  increases with the concentration of the target molecule. Other studies have shown similar results where higher  $R_{ct}$  was correlated with a higher concentration of redox species (glucose (Garcia-Hernandez et al., 2018), catechol (Sudeshna, Lang, & Bahadur, 2013), urea (Rajeswaran, Suni, Bever, & Hammock, 2014) were observed. Therefore, the EIS response would be affected by the interaction between the sensor and the analyte.

### 3.3. Analysis of milk using a bioelectronic tongue

Once the sensors and biosensors were characterized, they were implemented in a bioET for a first approach in milk analysis. The sensor array consisted of six sensors: one sensor modified with AgNPs and five biosensors modified with AgNPs and enzymes including galactose oxidase (GaOx), glucose oxidase (GOx), beta-galactosidase ( $\beta$ -Gal), urease (Ure) and lipase (Lip).

The impedimetric responses for the redox probe in the commercial milks are illustrated in Fig. 4. In all cases, Nyquist plots were characterized by an uncomplete depressed semicircle at high frequencies indicating that charge transfer controlled process followed by a linear region at lower frequencies corresponding to a diffusion process. In milks with different fat content the highest  $R_{ct}$  values were obtained for whole milk, while semi-skimmed and skimmed milk showed much similar results (Fig. 4A). This could be explained due to the interaction of the tryglicerids that would difficult the electron transfer process resulting in a higher  $R_{ct}$  values. If we observed the example of impedance curves obtained for whole milk adulterated with increasing concentrations of water the same effect is observed due to the reduction in the fatty acids concentration on sample. Moreover, these results prove how the system developed has the ability to determine difference between milk samples that have been diluted in water, which is one of the main adulterations faced in dairy industry (Fig. 4B.).

Fig. 4C shows the impedimetric responses of all the sensors developed in this work towards a lactose free milk sample. In this case we can observe how the biosensors modified with GaOx and GOx showed lower  $R_{ct}$  values than AgNPs sensors due to the enhanced redox activity of the enzymes. Furthermore, the urease modified sensor showed the highest  $R_{ct}$  this could be related to the low urea content in lactose free milks.

Therefore, according to the above results a higher  $R_{ct}$  would be related not only with the amount of tryglicerids of milk but also with a lower content of the enzymes target molecules. Additionally, this work shows that sensors can be employed as the sensing units of an impedimetric electronic tongue while having varying degrees of sensitivity.

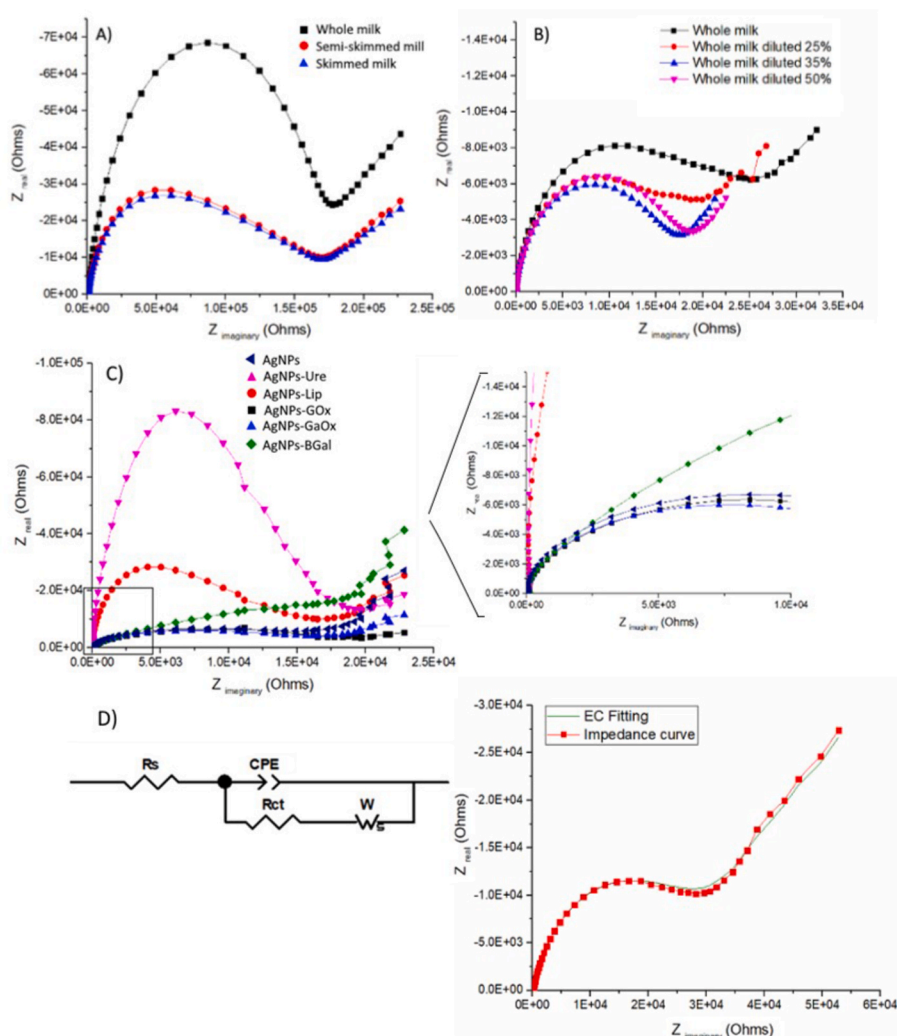


**Fig. 4.** A) Response of the AgNPs-GOx sensor to milks with different fat content. B) Response of the AgNPs-GaOx sensor to milks with different dilutions in water C) Response of the sensor array to lactose free whole milk. D) Equivalent physical electrical circuit applied and Impedance curve fitting.

Chemometric techniques were applied to analyze the outputs of the sensor array. Impedance spectra were processed using techniques to improve the accuracy of the feature extraction, as it is explained hereinafter. The traditional approach: choosing resistance/capacitance data at a set of frequencies as input data was used in the first statistical analysis. The impedance parameters selected were the real ( $Z_{REAL}$ ) and the imaginary ( $Z_{IMAGINARY}$ ) impedance data at 0.1, 1, 100, 1000, 10.000 and 100.000Hz taken from the Nyquist diagram as a wide representation of the different regions of the impedance analysis.

To carry out the second statistical, the impedance data for all milk samples were approximated to an equivalent physical electrical circuit (EC) using the methodology developed in a previous work (Garcia-Hernandez et al., 2018). This approximation allows to reduce the number of original variables in a new physical model formed by a series of electrical elements known as equivalent circuit. The difficulty of this approach lies in finding a single physical model capable of adjusting with low error values to all the signals recorded by the bioET, regardless of the sensor or the sample and to define the electrochemical, chemical, and physical procedures that take place at the electrode surface. The equivalent circuit used in this work is represented in Fig. 4C.

The proposed model, known as the Randles EC with diffusion, is widely employed to describe the behaviour of impedance based biosensors (Rajeswaran et al., 2014) for faradaic process. It is formed by different elements: the resistance associated to the solution,  $R_s$ , a

constant phase element, CPE dl, a charge transfer resistance,  $R_{ct}$ , and the Warburg impedance,  $W_s$ .

The high frequency region is dominated by the resistance of the solution ( $R_s$ ). In the mid-frequency region, the process is related to the formation of an electrical double layer at the film/solution interface.

The CPE represents a shift from the ideal capacitor behaviour instead of the typical capacitor in impedance spectroscopy; the depressed circle is an indication of this. The impedance of a CPE is defined as:

$$Z_{CPE} = \frac{1}{C(j\omega)^n} \quad (2)$$

where the imaginary unit is  $j$ ; when  $n = 0$ , the CPE describes an ideal resistor while when  $n = 1$  it is an ideal capacitor while  $C$  is a constant.

The charge transfer resistance ( $R_{ct}$ ) is related with two effects: the energy potential associated with oxidation/reduction processes and with the energy barrier of the redox species reaching the electrode.

Finally,  $W_s$  is a generalised finite Warburg element that its directly related with the diffusion of the mobile charge:

$$W_s = R_w \frac{\tanh(j\omega s)^n}{(j\omega s)^n} \quad (3)$$

where the diffusion resistance is represented by  $R_w$ , and  $s = \lambda^2/D$ ; where  $\lambda$  represents the effective diffusion thickness and  $D$  the operative diffusion coefficient.

In the case of faradaic impedance, the main parameters to be monitored are  $R_{ct}$  and  $R_w$ . The  $R_{ct}$  is mainly affected by the electron transfer kinetics from the electrolyte to the metal and depends on the properties of the redox probe and the interface structure. The use of electron mediators such as  $[Fe(CN)_6]^{4-/3-}$  at a sufficiently high concentration ensures that the charge transfer between the redox pair and the electrode surface does not limit the impedance so that the modification of the electrode surface in contact with the test medium causes its blocking and affects the  $R_{ct}$ .

The Warburg resistance,  $R_w$ , is related to the diffusion of the redox probe from the electrolyte to the interface. At high frequencies  $R_w$  is negligible since the diffusion path of the reagent species is very short, but at low frequencies the reagents have to diffuse farther increasing  $R_w$ .

Due to the high number of EC elements it was decided to choose only the resistances of the system as the input variables for the multivariate analysis. Therefore, a total of 15 variables (5 sensors x 3 resistors) will be included.

The results of the PCA analysis performed by using the parameters obtained from the impedance curves ( $Z_{REAL}$  and  $Z_{IMAGINARY}$ ) are shown in Fig. 5A. It was observed that discrimination between milk samples was dominated by their nutritional characteristics with very low influence of the different fat contents in the case of calcium enriched and lactose free milk. Furthermore, the explained variance from the original

data set only reached a 59% on their first two principal components (30%PC-1 and 29%PC-2) and up to 71% with the three first components (12% PC-3) without further clustering of the samples. Taking into account the low variance reached by the first two components the discrimination capability of the system can not be confirmed and should be further studied in this work.

As shown in Fig. 5B, in the case of PCA using EC parameters the explained variance on the first components for the bioET was 85%, distributed in 61% (PC-1) and 24% (PC-2) in the first two components. Moreover, a higher segregation of clusters can be observed. The diagram's right side showed lactose-free milk, while the center and left sides showed calcium-enriched milk and regular milk, respectively. This indicates that the first principal component is highly influenced by the nutritional content. Besides, classic milk and calcium-enriched milk show differentiated groups for whole, semi-skimmed and skimmed milk on the second principal component of the PCA. The multivariate analysis of impedimetric data reveals that the information extracted from the impedimetric curves can be upgraded by transforming EIS parameters into an EC model.

These results can be explained by the complexity of the curves obtained with the biosensors and the great cross-selectivity of the sensors included in the sensors array. Specific sensors for the detection of glucose, galactose, lactose and urea have a great influence on the

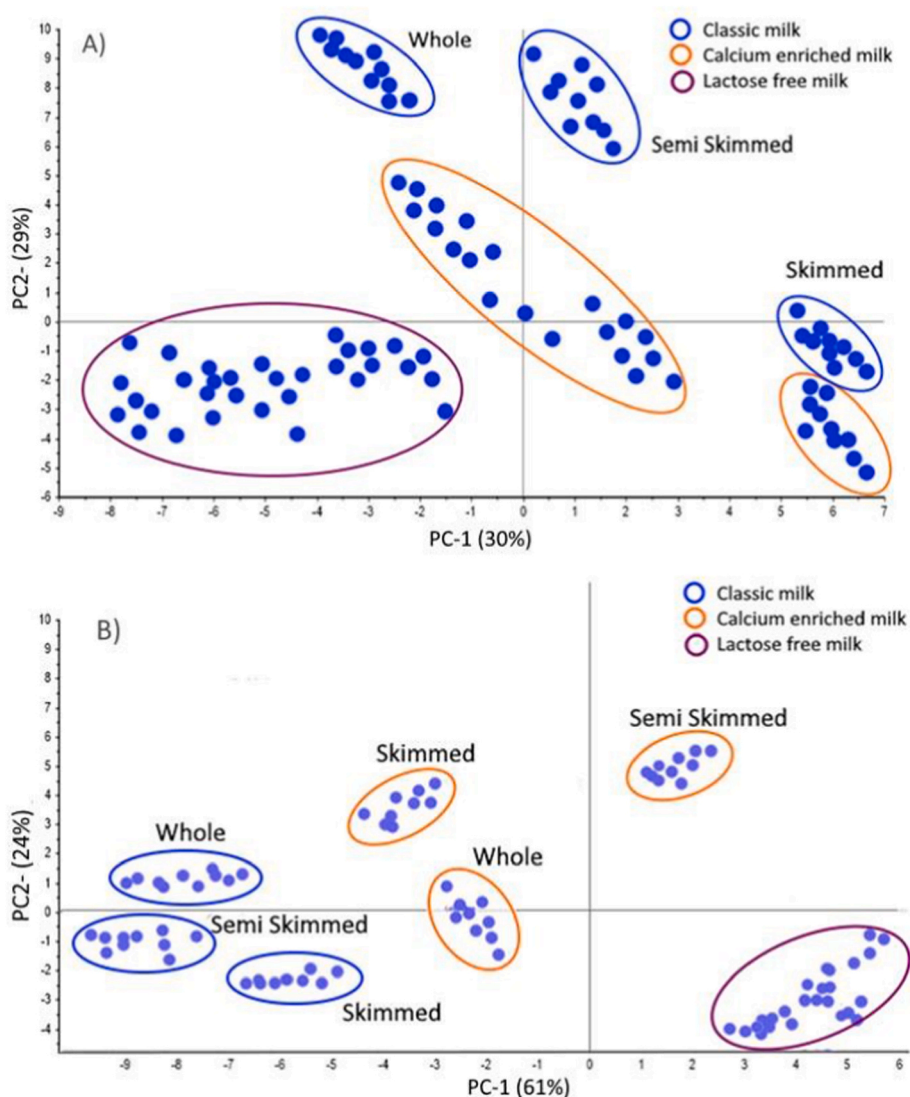


Fig. 5. A) PCA using the parameters obtained from the impedance curves B) PCA using EC parameters.

**Table 2**  
Confusion matrixes of the SVMC.

Nutritional content				
Training		Calcium	Classic	Lactose free
Calcium	Calcium	30 (100%)	0	0
	Classic	0	30 (100%)	0
	Lactose free	0	0	30 (100%)
Validation		Calcium	Classic	Lactose free
Calcium	Calcium	30 (100%)	0	0
	Classic	0	29 (100%)	0
	Lactose free	1 (4.75%)	0	30 (95.25%)
Fat content				
Training		Skimmed	Semi-Skimmed	Whole
Skimmed	Skimmed	30 (100%)	0	0
	Semi-skimmed	0	30 (100%)	0
	Whole	0	0	30 (100%)
Validation		Skimmed	Semi-Skimmed	Whole
Skimmed	Skimmed	30 (100%)	0	0
	Semi-skimmed	0	30 (100%)	0
	Whole	1(4.75%)	1(4.75%)	28 (90.5%)

discrimination capacity of the bioET, making it the source of the greatest variance in the system. While the sensor modified with AgNPs and the lipase biosensor provides information on the sample that is mainly related to their fat content.

Once the discrimination capability of the system was demonstrated, classification models were developed. To create a predictive classification model to classify milk samples into three groups (classic, calcium-enriched, and lactose free) support vector machine (SVMC) was used. Classification models were also built for the different fat contents: whole, semi-skimmed and skimmed milk. Both models were validated by tenfold cross validation, performing the validation method ten times, with each fitting being done on a training set made up of 90% of the entire training data set randomly chosen and the remaining 10% of the data being used as a hold out set for validation. The results of the second statistical approach are summarized in Table 2.

The SVMC model which was calculated from data collected using the bioET for milks with different nutritional contents produced recognition accuracy of 100% for all milk samples (error rate 0%) for the training by both statistical approaches. However, only 90.25% and 95.25% for the EC when it was validated using the impedance spectrum parameters ( $Z_{\text{REAL}}$  and  $Z_{\text{IMAGINARY}}$ ).

Both statistical approaches indicated that 100% of the samples were accurately classified into one of the three classes during the calibration phase for the fat content classification, while during the validation the accuracy achieved was only of 85.5% for the impedance spectrum parameters (error rate 14.5%) and 90.5% with an error rate of 9.5% in the case of the EC. This result reaffirmed the important role of the cross selectivity and biosensor influence in the performance of the bio-ET.

The impedimetric responses of the bio-ET and the physicochemical parameters (acidity, density, percentage of proteins, percentage of fats, percentage of lactose, percentage of DM, percentage of NFD, and urea) used to assess the quality of milk were then correlated using Support vector machine for regression (SVMR). Due to its ability to prevent overfitting and its capacity to manage non-linear interactions between

**Table 3**  
Correlation parameters of the SVMR using the impedance spectrum parameters ( $Z_{\text{REAL}}$  and  $Z_{\text{IMAGINARY}}$ ) and the EC as input data.

Parameters	$R_C^2$ (a)		RMSE <sub>C</sub> (b)		$R_V^2$ (c)		RMSE <sub>V</sub> (d)	
	$Z_{\text{REAL}}$ and $Z_{\text{IMAGINARY}}$	EC	$Z_{\text{REAL}}$ and $Z_{\text{IMAGINARY}}$	EC	$Z_{\text{REAL}}$ and $Z_{\text{IMAGINARY}}$	EC	$Z_{\text{REAL}}$ and $Z_{\text{IMAGINARY}}$	EC
Acidity	0.9023	0.9151	0.1157	0.1178	0.9002	0.9049	0.1187	0.1189
Density	0.9011	0.9013	0.1360	0.1370	0.8915	0.8909	0.1374	0.1394
%Proteins	0.9125	0.9242	0.1098	0.1079	0.9101	0.9041	0.1120	0.1086
%Fat	0.9215	0.9725	0.1028	0.1008	0.9121	0.9651	0.1078	0.1055
%Lactose	0.9218	0.9528	0.1136	0.1092	0.9203	0.9425	0.1145	0.1111
%DM	0.9125	0.9232	0.1245	0.1138	0.9017	0.9221	0.1258	0.1185
%NFD	0.9032	0.9312	0.1269	0.1141	0.9021	0.9203	0.1263	0.1151
Urea	0.9236	0.9612	0.1641	0.1581	0.9011	0.9409	0.1754	0.1693

sensor inputs and target properties, radial basis function was selected as the core function (Zhifeng, Wen, Yang, Lu, & Zhang, 2006). The kernel parameter ( $\gamma$ ) and penalty parameter ( $c$ ) of the radial basis function were optimized by a grid search methodology, where approaches to the mathematical model were made by  $\log_{10}c$  and  $\log_2\gamma$  with an epsilon of 0.1 in a range of [10,10]. The best validation accuracy for each of the systems developed was established when  $\gamma = 0.01$  combined with  $c = 1$ .

The statistical parameters obtained from the SVMR models are shown in Table 3. All of the parameters under consideration achieved good correlation coefficients ( $R^2$ ) and small residual errors (RMSE) for both calibration and prediction.

It is worth noting that, the regression using the EC parameters provided better correlations values and lower residual errors. Excellent correlations were obtained for fats, lactose and urea content. These values reflect the influence of biosensors capable of providing information on the sugar content (galactose, glucose and lactose) of the sample as well as the urea content of the analyzed samples. In addition, it is confirmed in this way that the global information of the sample has not been lost since very good correlations can be established with the fat content, the main component of milk capable of modifying the impedimetric response.

It is also significant that the bio-ET obtained a high correlation coefficient of 0.91 for the acidity value. This could be explained by the effect of acidity values related to the enzymatic response of the biosensors, since enzymes are highly affected by pHs.

The regression performed with the EC parameters provided the best correlations and had the lowest residual errors, confirming that the developed method enhances the quality of the features extraction.

#### 4. Conclusions

In this work, impedimetric biosensors were combined to develop a bioET applied in the analysis of milk samples with enhanced performance. Interdigitated sensors with higher concentrations of AgNPs showed greater sensitivity towards compounds of interest such as glucose, galactose, lactose, urea and triglycerides while the utilization of enzymes allowed a remarkable increase in the system specificity. These results demonstrate that the presence of AgNPs allows a higher electron transfer on the sensors surface increasing the signals provided by the interaction of the sample with sensor. Moreover, this higher electron transfer improves the detection of the catalytic activity of the enzymes inducing distinctive performance characteristics in terms of sensitivity.

Furthermore, two sadistic approaches were tested in the data processing, using the resistance/capacitance data at a set of frequencies as input data and the resistance data obtained in the adjustment to EC. Principal component analysis demonstrated that the bioET combining AgNPs and enzymes was capable to discriminate between commercial milk samples (classic, calcium and lactose free) according to their nutritional composition with a much better performance in the case of the EC approach that was able to reach up to 85% of explained variance in the first two components of the model compared with the 71% reached on three components by the first statistical approach. Furthermore, excellent correlations with the chemical parameters commonly



used in the milk quality control milk were found using SVM. This result confirms that the benefits of multisensory systems that offer global information are maintained while the biosensors boost the specificity of electronic tongue nanoparticles. Although both statistical approaches had good results the use of the resistance data from the EC as the input data appears to be a better choice due to the higher correlations with up to a 0.942, 0.94 and 0.96 in the case of lactose, urea and fat content prediction. These results demonstrated that the bioelectronic tongue developed in combination with the equivalent circuits approach for data processing could be a potential tool for its further application in dairy analysis.

## Funding

This work was supported by MICINN-FEDER (PID2021-122365OB-I00), «Infraestructuras Red de Castilla y Leon (INFRARED)» and JCyL Consejería de Educación - FEDER (VA275P18). We would also like to thank the Calidad Pascual farm (Aranda de Duero) for the loan of samples (ALIVAC-IDI-20211051).

## Authors contribution

CG-C, MR-M and FM-P conceptualized the idea and supervised the work. CP-G and CS-C carried on the experiments, processed the data and wrote the original paper draft. FM-P was involved in the design of the software. CP-G and CS-C were involved in data analysis. CG-C and MR-M acquired the funding. All authors reviewed and edited the paper. All authors provided feedback.

## Declaration of competing interest

The authors declare that they have no known competing financial interests or personal relationships that could have appeared to influence the work reported in this paper.

## Data availability

Data will be made available on request.

## References

- Ali Saad, E. A., Wadood, S. A., & Ali, A. K. (2019). Development of Hydrogen peroxide biosensor based on immobilization of Hemoglobin on screen-printed carbon electrode modified with silver nanoparticles. *I. Journal of Science*, 2332–2340. <https://doi.org/10.24996/ij.s.2019.60.11.3>
- Creighton, J. A., Blatchford, C. G., & Albrecht, M. G. (1979). Plasma resonance enhancement of Raman scattering by pyridine adsorbed on silver or gold sol particles of size comparable to the excitation wavelength. *Journal of the Chemical Society, Faraday Transactions*, 75(2), 790–798. <https://doi.org/10.1039/F29797500790>
- Daniels, J. S., & Pourmand, N. (2007). Label-free impedance biosensors: Opportunities and challenges. *Electroanalysis*, 19(12), 1239–1257. <https://doi.org/10.1002/elan.200603855>
- Eugenii, K., & Willner, I. (2003). Probing biomolecular interactions at conductive and semiconductive surfaces by impedance spectroscopy: Routes to impedimetric immunosensors, DNA-sensors, and enzyme biosensors. *Electroanalysis*, 15(11), 913–947. <https://doi.org/10.1002/elan.200390114>
- Fernanda, M. L., Sanfelice, R. C., Mercante, L. A., Andre, R. S., Mattoso, L. H. C., & Correa, D. S. (2018). Urea impedimetric biosensing using electrospun nanofibers modified with zinc oxide nanoparticles. *Applied Surface Science*, 443, 18–23. <https://doi.org/10.1016/j.apsusc.2018.02.168>
- Garcia-Hernandez, C., Salvo-Comino, C., Martín-Pedrosa, F., Rodríguez-Mendez, M. L., & García-Cabezon, C. (2018). Impedimetric electronic tongue based on nanocomposites for the analysis of red wines. Improving the variable selection method. *Sensors and Actuators B: Chemical*, 277, 365–372. <https://doi.org/10.1016/j.snb.2018.09.023>
- Garcia-Hernandez, C., Salvo-Comino, C., Martín-Pedrosa, F., García-Cabezon, C., & Rodríguez-Mendez, M. L. (2020). Analysis of red wines using an electronic tongue and infrared spectroscopy. Correlations with phenolic content and color parameters. *Lebensmittel-Wissenschaft und -Technologie*, 118, Article 108785. <https://doi.org/10.1016/j.lwt.2019.108785>
- Goran, S. M., Sinha, A., Ali, A. E., Jeoti, V., Radoičić, M. B., Marković, D. D., et al. (2021). Impedance analysis of milk quality using functionalized polyamide textile-based sensor. *Computers and Electronics in Agriculture*, 191, Article 106545. <https://doi.org/10.1016/j.compag.2021.106545>
- Govindhan, M., & Jin, W. (2017). Nanomaterials based electrochemical sensor and biosensor platforms for environmental applications. *Trends in Environmental Analytical Chemistry*, 13, 10–23. <https://doi.org/10.1016/j.teac.2017.02.001>
- Hui, X., Gorgy, K., Gondran, C., LeGoff, A., Spinelli, N., Lopez, C., et al. (2013). Label-free impedimetric thrombin sensor based on poly(pyrrole-nitrotriacetic acid)-aptamer film. *Biosensors and Bioelectronics*, 4, 90–95. <https://doi.org/10.1016/j.bios.2012.07.044>
- International Organization For Standardization. (2021). *ISO/TC 34/SC 5 - milk and milk*.
- Joung, C., Kim, H., Lim, M., Jeon, T., Kim, H., & Kim, Y. (2013). A nanoporous membrane-based impedimetric immunosensor for label-free detection of pathogenic bacteria in whole milk. *Biosensors and Bioelectronics*, 44, 210–215. <https://doi.org/10.1016/j.bios.2013.01.024>
- Kelcilene, T. B. R., Flávio, M. S., Scagion, V. P., & Correa, D. S. (2019). Ternary nanocomposites based on cellulose nanowhiskers, silver nanoparticles and electrospun nanofibers: Use in an electronic tongue for heavy metal detection. *Sensors and Actuators B: Chemical*, 290, 387–395. <https://doi.org/10.1016/j.snb.2019.03.125>
- Kelcilene, T. B. R., Shimizu, F. M., Scagion, V. P., & Correa, D. S. (2019). Ternary nanocomposites based on cellulose nanowhiskers, silver nanoparticles and electrospun nanofibers: Use in an electronic tongue for heavy metal detection. *Sensors and Actuators B: Chemical*, 290, 387–395. <https://doi.org/10.1016/j.snb.2019.03.125>
- Lopes, A. L. M., Machado, J. A., Ramalho, E., & Silva, V. (2017). Milk characterization using electrical impedance spectroscopy and fractional models. *Food Analytical Methods*, 11(3), 901–912. <https://doi.org/10.1007/s12161-017-1054-4>
- Luka, G., Ahmadi, A., Najjaran, H., Alocilja, E., DeRosa, M., Wolthers, K., et al. (2015). Microfluidics integrated biosensors: A leading technology towards lab-on-a-chip and sensing applications. *Sensors*, 15(12), 30011–30031. <https://doi.org/10.3390/s151229783>
- Manzoli, A., Shimizu, F. M., Mercante, L. A., Paris, E. C., Oliveira, O. N., Correa, D. S., et al. (2014). Layer-by-layer fabrication of AgCl-PANI hybrid nanocomposite films for electronic tongues. *PCCP: Physical Chemistry Chemical Physics*, 16(44), 24275–24281. <https://doi.org/10.1039/c4cp04150j>
- Masot, R., Alcañiz, M., Fuentes, A., Schmidt, F. C., Barat, J. M., Gil, L., et al. (2010). Design of a low-cost non-destructive system for punctual measurements of salt levels in food products using impedance spectroscopy. *Sensors and Actuators A: Physical*, 158(2), 217–223. <https://doi.org/10.1016/j.sna.2010.01.010>
- Mercante, L. A., Scagion, V. P., Pavinatto, A., Sanfelice, R. C., Mattoso, L. H., & Correa, D. S. (2015). Electronic tongue based on nanostructured hybrid films of gold nanoparticles and phthalocyanines for milk analysis. *Journal of Nanomaterials*, 2015, 1–7. <https://doi.org/10.1155/2015/890637>
- Murilo, F. H. M., Mercante, L. A., Mattoso, L. H. C., & Correa, D. S. (2017). Detection of trace levels of organophosphate pesticides using an electronic tongue based on graphene hybrid nanocomposites. *Talanta*, 167, 59–66. <https://doi.org/10.1016/j.talanta.2017.02.005>
- Park, J. S., Grijalva, S. I., Aziz, M. K., Chi, T., Li, S., Sayegh, M. N., et al. (2018). Multi-parametric cell profiling with a CMOS quad-modality cellular interfacing array for label-free fully automated drug screening. *Lab on a Chip*, 18(19), 3037–3050. <https://doi.org/10.1039/c8lc00156a>
- Park, J., Kim, H., Lee, J., Park, J., Kim, J., Hwang, K., et al. (2018). Amyloid beta detection by faradaic electrochemical impedance spectroscopy using interdigitated microelectrodes. *Sensors*, 18(2), 426. <https://doi.org/10.3390/s18020426>
- Pérez-González, C., Salvo-Comino, C., Martín-Pedrosa, F., García-Cabezon, C., & Rodríguez-Méndez, M. L. (2023). Bioelectronic tongue dedicated to the analysis of milk using enzymes linked to carboxylated-PVC membranes modified with gold nanoparticles. *Food Control*, 145, Article 109425. <https://doi.org/10.1016/j.foodcont.2022.109425>
- Rajeswaran, R., Suni, I. I., Bever, C. S., & Hammock, B. D. (2014). Impedance biosensors: Applications to sustainability and remaining technical challenges. *ACS Sustainable Chemistry & Engineering*, 2(7), 1649–1655. <https://doi.org/10.1021/sc500106y>
- Reis, R. M., Valim, R. B., Rocha, R. S., Lima, A. S., Castro, P. S., Bertotti, M., et al. (2014). The use of copper and cobalt phthalocyanines as electrocatalysts for the oxygen reduction reaction in acid medium. *Electrochimica Acta*, 139, 1–6. <https://doi.org/10.1016/j.electacta.2014.07.003>
- Riul, A., Malmegrim, R. R., Fonseca, F. J., & Mattoso, L. H. C. (2003). An artificial taste sensor based on conducting polymers. *Biosensors and Bioelectronics*, 18(11), 1365–1369. [https://doi.org/10.1016/s0956-5663\(03\)00069-1](https://doi.org/10.1016/s0956-5663(03)00069-1)
- Salvo-Comino, C., Martín-Bartolomé, P., Pura, J. L., Perez-Gonzalez, C., Martín-Pedrosa, F., García-Cabezon, C., et al. (2022). Improving the performance of a bioelectronic tongue using silver nanowires: Application to milk analysis. *Sensors and Actuators B: Chemical*, 364, Article 131877. <https://doi.org/10.1016/j.snb.2022.131877>
- Sandeep, S., Santhosh, A. S., Swamy, N. K., Suresh, G. S., & Melo, J. S. (2019). Detection of catechol using a biosensor based on biosynthesized Silver Nanoparticles and Polyphenol Oxidase Enzymes. *Electrochimica Acta*, 37(4), 257–270. <https://doi.org/10.4152/pea.201904257>
- Shrikrishnan, S., & Lakshminarayanan, V. (2012). Electron transfer studies of redox probes in bovine milk. *Journal of Colloid and Interface Science*, 370(1), 124–131. <https://doi.org/10.1016/j.jcis.2011.12.070>
- Siuli, D., Sivaramakrishna, M., Biswas, K., & Goswami, M. (2011). Performance study of a 'constant phase angle based' impedance sensor to detect milk adulteration. *Sensors and Actuators A: Physical*, 167(2), 273–278. <https://doi.org/10.1016/j.sna.2011.02.041>

- Skládal, P. (2020). Smart bioelectronic tongues for food and drinks control. *Trends in Analytical Chemistry*, 127, Article 115887. <https://doi.org/10.1016/j.trac.2020.115887>
- Sobrinho-Gregorio, L., Bataller, R., Soto, J., & Escriche, I. (2018). Monitoring honey adulteration with sugar syrups using an automatic pulse voltammetric electronic tongue. *Food Control*, 91, 254–260. <https://doi.org/10.1016/j.foodcont.2018.04.003>
- Sudeshna, C., Lang, H., & Bahadur, D. (2013). Polyaniline-iron oxide nanohybrid film as multi-functional label-free electrochemical and biomagnetic sensor for catechol. *Analytica Chimica Acta*, 795, 8–14. <https://doi.org/10.1016/j.aca.2013.07.043>
- Sun, L., Zhang, S., Li, Q., Yuan, E., Chen, R., Yan, F., et al. (2023). Metabolomics and electronic tongue reveal the effects of different storage years on metabolites and taste quality of Oolong Tea. *Food Control*, 152, Article 109847. <https://doi.org/10.1016/j.foodcont.2023.109847>
- Swatland, H. J., Darkin, F., Naylor, S. J., Caston, L., & Moccia, R. D. (1998). Muscle colour development in Arctic charr, *Salvelinus alpinus* (L.), monitored by fibre-optics and electrical impedance. *Aquaculture Research*, 29(5), 367–372. <https://doi.org/10.1111/j.1365-2109.1998.00211.x>
- Tolga, K., Ates, M., & Sarac, A. S. (2016). Covalent immobilization of urease on poly (pyrrole-3-carboxylic acid): Electrochemical impedance and mott Schottky study. *Journal of the Electrochemical Society*, 163, 8. <https://doi.org/10.1149/2.0671608jes>
- Ulloa, P. A., Guerra, R., Cavaco, A. M., da Costa, A. M. R., Figueira, A. C., & Brigas, A. F. (2013). Determination of the botanical origin of honey by sensor fusion of impedance e-tongue and optical spectroscopy. *Computers and Electronics in Agriculture*, 94, 1–11. <https://doi.org/10.1016/j.compag.2013.03.001>
- Vanessa, S. P., Mercante, L. A., Sakamoto, K. Y., Oliveira, J. E., Fonseca, F. J., Mattoso, L. H., et al. (2016). An electronic tongue based on conducting electrospun nanofibers for detecting tetracycline in milk samples. *RSC Advances*, 6(105), 103740–103746. <https://doi.org/10.1039/c6ra21326j>
- Veiga, E. A., & Bertemes-Filho, P. (2012). Bioelectrical impedance analysis of bovine milk fat. *Journal of Physics: Conference Series*, 407, Article 012009. <https://doi.org/10.1088/1742-6596/407/1/012009>
- Wang, Y., Ping, J., Ye, Z., Wu, J., & Ying, Y. (2013). Impedimetric immunosensor based on gold nanoparticles modified graphene paper for label-free detection of *Escherichia coli* O157:H7. *Biosensors and Bioelectronics*, 49, 492–498. <https://doi.org/10.1016/j.bios.2013.05.061>
- Wania, C. A., Shimizu, F. M., Fature, M. H. M., Cerri, R., Oliveira, O. N., Correa, D. S., et al. (2021). Two-dimensional MoS<sub>2</sub>-based impedimetric electronic tongue for the discrimination of endocrine disrupting chemicals using machine learning. *Sensors and Actuators B: Chemical*, 336, Article 129696. <https://doi.org/10.1016/j.snb.2021.129696>
- Xiliang, L., Morrin, A., Killard, A. J., & Smyth, M. R. (2006). Application of nanoparticles in electrochemical sensors and biosensors. *Electroanalysis*, 18(4), 319–326. <https://doi.org/10.1002/elan.200503415>
- Zhifeng, H., Wen, W., Yang, X., Lu, J., & Zhang, G. (2006). A fast data preprocessing procedure for support vector regression. *Intelligent Data Engineering and Automated Learning – IDEAL*, 48–56. [https://doi.org/10.1007/11875581\\_6](https://doi.org/10.1007/11875581_6)
- Clara Perez-Gonzalez obtained the Ms in Nanoscience in 2019 (U. Valladolid. Spain). She is currently working on her PhD Thesis which is dedicated to the development of electrochemical sensors for the analysis of foods. She is author of 5 scientific papers.
- Coral Salvo-Comino obtained her PhD dedicated to the development of electrochemical sensors for the analysis of foods in July 2022 (U. Valladolid. Spain). She is author of 16 scientific papers in the field.
- Fernando Martin-Pedrosa is full professor at the University of Valladolid and Head of the Department of Materials Science. His research is dedicated to electrochemistry studies of different solid materials. He is author of more than 80 papers.
- Cristina Garcia Cabezon, is assistant professor at the Engineers school of the University of Valladolid. She is an expert in electrochemistry and impedance spectroscopy. She is author or coauthor of more than 60 papers in the field.
- Maria Luz Rodriguez-Mendez is Full professor of Inorganic Chemistry at the Engineers School of the University of Valladolid and Head of the group of sensors UVASens. She is leading several funded Projects devoted to the development of arrays of voltammetric nanostructured sensors and biosensors for the characterization of foods. She is author or co-author of over 165 publications (H index 44), seven books and three patents in the field.